Engineering Conferences International
ECI Digital Archives

5th International Conference on Porous Media and Their Applications in Science, Engineering and Industry

Refereed Proceedings

MRI evidence of nanoparticles migration in drying porous media

Emmanuel Keita
Université Paris-Est

Pamela faure
Université Paris-Est

Stephane Rodts
Université Paris-Est

Phillippe Coussot
Université Paris-Est

Follow this and additional works at: http://dc.engconfintl.org/porous_media_V

Part of the Materials Science and Engineering Commons

Recommended Citation

MRI EVIDENCE OF NANOPARTICLES MIGRATION IN DRYING POROUS MEDIA

Emmanuel Keita, Paméla Faure, Stéphane Rodts and Philippe Coussot
Université Paris-Est, Laboratoire Navier, Champs sur Marne, 77420, France

keita.emmanuel@gmail.com

ABSTRACT

Due to the migration of elements they induce imbibition-drying cycles are known to play a major role in the colloid-facilitated transport in many industrials process, for instance for pollutants migration in soils or pores clogging in building materials.

We study the drying of a colloidal suspension in a porous media. The critical physical phenomenon at work here is the displacement and redistribution of colloidal particles induced by evaporation of the liquid phase from the porous medium.

This can be clearly seen by filling a bead packing with coffee. Indeed after full drying the sample has shaded tones with darker regions around the sample free surface and white regions almost free of particles around the bottom. The mechanisms are not yet fully understood and there is no straightforward observation and simple quantification of the spreading of the elements.

To better understand the phenomenon, we perform the same experiment using with a clear scaling separation between the porous structure (glass beads diameter=200 µm) and nanoparticles in suspension in water (diameter = 20 nm). Using a new MRI technique to measure the distributions of water and particles we observe particles rising towards the free surface, as water remains homogenously distributed. The particles aggregation area is very large compare to their volume fraction in the pore volume. But we can quantify how the elements migrate towards the free surface of the sample and accumulate in the remaining liquid films. Our complete understanding of the process makes it possible to establish a simple model predicting the drying rate and the concentration distribution [7]. This opens the way to a control of salt or colloid migration and drying rate of soils and building materials.
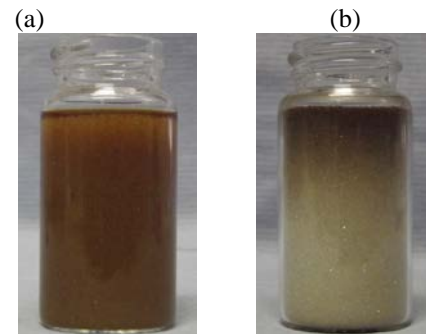
INTRODUCTION

Figure 1: Porous medium made of glass beads packing homogeneously filled with a coffee suspension before (a) and after (b) drying under natural room convection and ambient temperature.

After drying a coffee suspension initially homogeneously dispersed in a porous medium (white glass bead packing) a surprising concentration gradient appears (see Fig.1). The initially black sample (see Figure 1a) has finally shaded tones with darker regions around the sample free surface and white regions almost free of particles around the bottom (see Figure 1b). Thus coffee particles have moved from the bottom to the upper layers during the drying process, which suggests that they are transported with the liquid towards the free surface.

Such a situation in which a porous medium filled with a suspension dries is extremely frequent in industry and nature. It plays a major role in the colloid-facilitated transport of pollutants through soils [6], salt crystallization leading to deterioration of building materials [11-12], clogging of road surfaces [5], and evolutions of soil fertility and workability [17]. However, as far as we know, whereas the behavior of ion solutions in drying porous media has been fairly investigated, there is no straightforward observation and quantification of the colloid dynamics under such conditions and the phenomenon described above has not been mentioned.

Colloidal particles dynamics in drying droplets has been widely explored. In particular it has been shown that a coffee-ring effect occurs as a result of particle

accumulation towards the contact line [2]. The corresponding dry front progression has been directly observed in thick films of colloidal suspension [8] and through deposits of dye at the drying spots in porous media [15]. Further studies showed how this effect may be suppressed, mainly through Marangoni flows (temperature, solvent mixture), or more surprisingly by changing the particle shape. Besides it was shown that at high concentration a solid phase forms that can buckle or crack due to high capillary stresses [3, 9,10,16], and that advection-diffusion models predict well the colloid accumulation in liquid droplets or salt solution in porous media [11-12].

One knows that simple liquid evaporates from porous medium through a succession of regimes [19] including mainly a first stage of liquid redistribution via capillary effects (constant rate period) [18] and a second stage of dry front penetration (falling rate period). The impact of the presence of solid additives in the liquid has not been taken into account, in particular due to the difficulty to obtain accurate measurements of the evolution of the colloidal phase inside the porous medium. MRI is a powerful tool to look into opaque materials which has been used to measure either the water distribution or phase changes inside porous media [11-13] or the solid concentration in colloidal systems. However, the usual unique MRI signal cannot account for the multiphasic nature of a colloidal system in a porous medium. In this letter, we study such systems with a new MRI protocol to observe at the same time the distribution or air, liquid and colloid through the unsaturated solid porous structure. We show that the drying process relies on a new general phenomenon: a receding coffee-front effect. The elements migrate towards the free surface of the sample and accumulate in the remaining liquid films, which leads to a continuous decrease in concentration from the top to the bottom of the sample at the end of drying. Our understanding of the process makes it possible to establish a simple model predicting the drying rate and the concentration distribution [7].

NOMENCLATURE

a	=	Bead radius
D	=	Diffusion coefficient
J	=	Rate of drying
k_B	=	Boltzmann constant
n_{sat}	=	Maximum vapour density
R	=	Particles Radius
$R_{surface}$	=	Surface relaxation
S	=	Contact surface area between solid and liquid phases
s	=	Wetted surface area to pore volume ratio
V	=	Drying velocity
V_d	=	Characteristic diffusion velocity
V_f	=	Capillary pressure velocity
V_l	=	Fluid volume
T	=	Temperature (° Kelvin)
T_1	=	NMR Relaxation time
z	=	Size of the compacted front

Greek Symbols

α	=	Calibration constant of the particle contribution to NMR relaxation
β	=	Second Letter in Greek Alphabet
γ	=	Surface tension
δ	=	Initial equivalent diffusion length
λ	=	Characteristic length of particles accumulation
ρ	=	Surface relaxivity
$ρ_0$	=	Liquid density
ϕ	=	Ratio of the water volume to the available pore volume
χ	=	Volume fraction of colloids in the pores
ψ	=	Volume fraction of colloidal particles in the liquid (water + particles) phase
ω	=	Porosity

1 MRI colloidal concentration determination

Beyond the first illustration above it is critical to observe the physical processes inside the sample, in particular the liquid and particle motions. In that aim, instead of coffee we used hydrophilic colloidal silica nanoparticles (Ludox HS-40 diameter: 20 nm) suspended in water at initial volume fractions (ψ_0) ranging from 0 to 15%, and we carried out tests with the same beads (packed by hand) in a cylindrical sample under stream of dehydrated air at ambient temperature along the top surface. While the water evaporates we follow the local water saturation in the porous medium (ϕ) and the volume fraction of colloids in the pores χ. We can then compute the local volume fraction of colloidal particles in the liquid (water + particles) phase: $\psi = \chi /(\chi + \phi)$.

In that aim the distribution of apparent water along the sample axis was measured by a ^{1}H MRI spectrometer with a one-dimensional double spin-echo. Each measured value of this distribution thus corresponds to the total amount of water in a thin cross-sectional layer situated at a given position along the sample axis. The determination of local particle concentrations relies on local measurements of water spin-lattice relaxation time T1 using a conventional series of T1-weighted spin-echo profiles. As compared with free water (which from our MRI system has a relaxation time $T_{1,bulk}$ =2.5s), relaxation in our samples is enhanced due to contacts with beads and particles. Provided molecular exploration of the porous network owing to Brownian motion is faster than local relaxation processes the observed relaxation rate $1/T_1$ is the sum of individual contributions from bulk relaxation process, water-bead and water-particle contact relaxations. Since relaxation at solid surfaces is reliably [4] described as

$R_{surface} = \rho S / V_l$, we can finally write the relaxation rate in our unsaturated porous system as

$$\frac{1}{T_1} \approx \frac{1}{T_{1,bulk}} + \frac{\rho s}{\phi} + \alpha \frac{\chi}{\phi} \qquad (1)$$

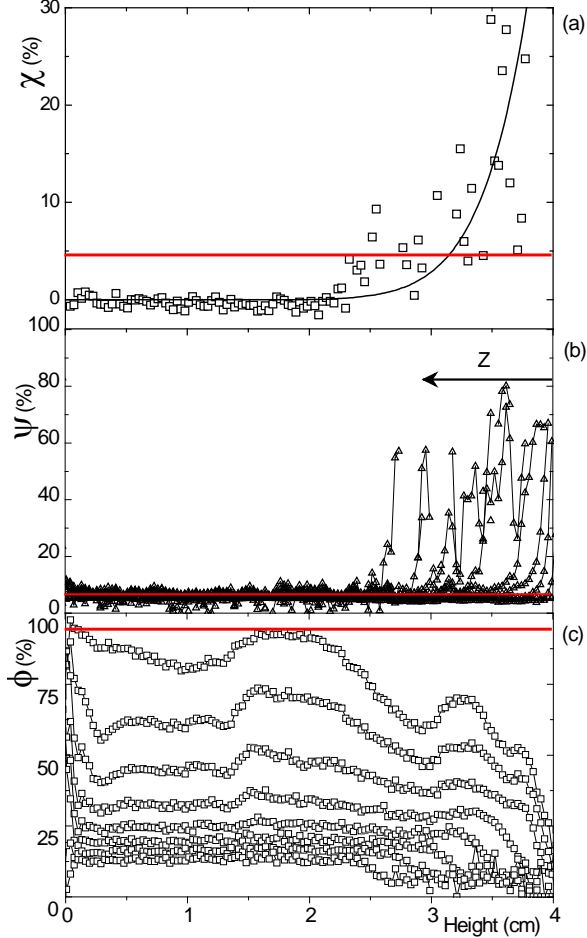## 2 Compaction front and capillary reequilibration

Figure 2: Drying of a cylindrical porous medium made of glass beads initially filled with a colloidal suspension at 5% volume fraction in water. Drying occurs through the upper surface (right). (a) distribution of particles in the pores at the end of the experiment (the black line corresponds to equation (4)), (b) distribution of colloids in the liquid phase and (c) distribution of water as a function of sample height. For the two last figures the profiles displayed are separated by 10 hours. Red thick lines represent the initial state.

Let us now look at the distribution of colloidal particles in the sample. Although it was initially homogeneous, at the end of the drying the distribution is strongly heterogeneous (see Figure 2a): despite the data scattering we clearly see that the concentration is around zero over some significant thickness then increases and reaches a value much larger than the initial one around the free surface of the sample. Such a distribution is qualitatively similar to the apparent one for the sample filled with coffee.

These data suggest that the effect observed for the coffee in the bead packing is general: the colloidal particles tend to move towards the free surface of the sample. Finally there is a kind of coffee ring effect in a porous medium but here the colloidal particles do not accumulate essentially at the edge of the sample, they are dispersed throughout some part of the sample.

Although for salt solutions diffusion can play a significant role [11-12], this is not the case here with nanoparticles since the Peclet number (i.e. V/V_d) is very large. We are in the advection regime [2]: as soon as some liquid is withdrawn somewhere the particles do not have time to redistribute homogeneously in the liquid by diffusion because the characteristic diffusion velocity is smaller than the velocity of advancement of the front. The drying front velocity, equal to the drying rate expressed in the form of a velocity, i.e. $V = (1/\rho_0 S) \mathrm{d} m / \mathrm{d} t$ with m the total sample mass, ρ_0 the liquid density and S the sample cross-section, is larger than the characteristic diffusion velocity of a colloidal particle over the sample height (H) which expresses as $V_d = k_B T / \pi \mu R H$ in which μ is the liquid viscosity and R the particle radius. We have $V_d \approx 3.10^{-9}$ m.s^{-1} while in our tests V ranges from 10^{-6} m.s^{-1} to 10^{-8} m.s^{-1}.

In order to understand how this distribution forms it is instructive to look at the evolution of the concentration of colloidal particles in the liquid phase. It appears that this concentration remains equal to the initial one in some (lower) region while it becomes equal to slightly more than 60% in an upper region of thickness growing in time (see Figure 2b). Such a concentration value is close to the maximum packing fraction of uniform spheres. Thus the process develops in the form of a *compacted front* progressing (receding) inside the sample. Note that in this region the pores are not saturated with a concentrated suspension, this is the remaining suspension volumes which are filled with colloidal particles (at the maximum packing fraction).

It is remarkable that in this compacted front the water saturation is very low whereas, below this region, it remains at a relatively high and almost uniform level which continuously decreases in time as the compacted front progresses (see Figure 2c). Such a horizontal profile over the whole sample and decreasing in time is usually observed when drying porous media saturated with a simple liquid [11,12, 14]. It is associated with a capillary re-equilibration process while the water evaporates essentially along the free surface of the sample. The origin of this effect is now well known: withdrawing water along the free surface creates menisci which induce a capillary depression (scaling as γ/a)

tending to move upwards the liquid situated beneath via some global capillary re-equilibration process of the liquid network throughout the sample [1]. This process occurs as bursts [18] which allow for air penetration in the largest pores whatever their position in the sample. By this means the water moves towards the free surface in the liquid state. Since during this stage the whole sample remains wet the air inside the sample is saturated with vapour, which precludes any evaporation process. As a consequence the drying mainly results from evaporation along the liquid-air interfaces at the top of the sample, which are close to the ambient air in which the vapour density is generally much lower. This explains that the rate of drying remains almost constant as long as a capillary re-equilibration can occur, i.e. as long as the rate of evaporation is smaller than the rate of the flow in the liquid films induced by capillary effects. Since the latter phenomenon results from the liquid flow through a liquid network with channels of size proportional to a under the action of the above capillary pressure the corresponding velocity (V_f) scales as $\beta\gamma R/\mu H$, in which H is the sample height, and β a coefficient related to the structure of the liquid network which is of the order of 0.002 for a saturated bead packing [1]. Thus here V_f is of the order of 10^{-5} m.s^{-1}, which is much larger than the drying velocity in our tests. This implies that in our case capillary re-equilibration is dominant in the wet region as long as the saturation is not too low.

In the compacted region there is still some water in the pores of this colloidal particle packing. However this water is trapped in nanopores (~3 nm) from which it does not easily escape. In particular its evaporation would lead to the exposure of the solid surface of colloid to air, which is not energetically favourable. This Kelvin effect suggests that the water in such pores may be at equilibrium with an external vapour density much smaller than 100%. Moreover the liquid flow velocity under capillary pressure effect (V_f) is now of the order of 10^{-9} m.s^{-1}, much smaller than the drying velocity of our samples. We conclude that the liquid trapped in the compacted front then remained essentially static during the rest of the experiment; it negligibly takes part to the drying process of the rest of the sample. As a consequence it is likely that drying occurs via the evaporation from the upper surface of the uncompacted (wet) region then diffusion through some air network towards the free surface of the sample.

3 Model of colloidal drying in porous media

As a consequence the picture which emerges is as follows. The colloidal particles are transported with the liquid which is drained by capillary effects towards the free surface, where they store and start to form a compacted region. The drying then results from evaporation along the upper free surface of the wet region in the bead packing, i.e. just below the compacted front. This explains why the drying rate decreases and there is no constant rate period (see Figure 3). During this process the water in the wet region is still drained by capillary process towards the lower surface of the compacted front. Let us recall that although the particle concentration in the water volume is at its maximum value (around 60%) in the compacted region the volume fraction of suspension (water + particles) in the pores decreases downwards. Thus there is an air network starting from the free surface and with a corresponding concentration increasing downwards. This network allows for vapour diffusion from the upper surface of the wet region. In the bottom part, the saturation decreases and the colloidal concentration is low (close to the initial one); thus the volume fraction of colloids in the pore drops to zero, and the process removes the particles from the bottom.

Our assumption about the main evaporation process taking place below the compacted region is confirmed by the fact that we can predict the rate of drying assuming diffusion over a distance equal to the measured thickness (z, see Figure 2.b.) of the compacted front. The rate of drying ($J = \rho_0 V/\omega$) may be found from the diffusion equation [1] $J \approx D n_{sat}/(\delta + z)$, in which D is the diffusion coefficient of water through the air ($D_{water} = 2.7\,10^{-5}\,\mathrm{m}^2.\mathrm{s}^{-1}$), $n_{sat} = 23.4$ g.m^{-3}. Using the (measured) size (z) of the compacted front in time (see Figure 2b) we computed the drying rate in time and thus the evolution of the water saturation. It appears that this model is in good agreement with the data which confirms the validity of our physical scheme, but some significant discrepancy is observed at concentrations larger than 15% (see dotted lines in Figure 3).
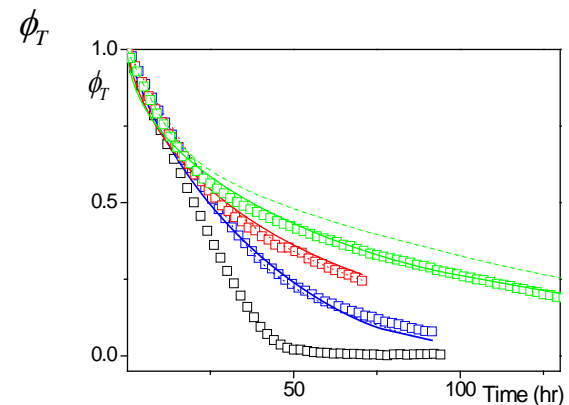

Figure 3: Total water saturation (ratio of the total mass of water to the initial mass **of water**) as a function of time during the drying of a porous medium. Initially filled with: (black) pure water, (blue) 5% colloidal particles in water, (red) 10%, (green) 15%. The square symbols correspond to the experimental data. The dotted lines correspond to the modelling approach based on the

measure of the compacted front thickness, and the continuous lines to the full modelling approach.

We can now use all our knowledge of the process to develop a full modelling approach predicting the evolution of the rate of drying and the final distribution of particles without any measurement. As the particles act as markers of the fluid, due to the water arrival from below they accumulate and pack at $\psi_m \approx 60\%$, leading to an increase of the compacted region (of size z). The growth of this region is related to the drying rate via:

$$\psi_0 (1 - \psi_0) J = \phi (\psi_m - \psi_0) \dot{z} \qquad (2)$$

Simultaneously, the bottom part of the sample (still liquid), which provides the evaporative water, desaturates homogenously so that the drying rate is also related to the saturation change in this region:

$$(1 - \psi_0) J = -(H - z) \dot{\phi} \qquad (3)$$

Dropping J from these two equations we get a differential equation which may be solved to find the relationship between the front advancement and the saturation. We can in particular deduce the final distribution of particles as a function of the depth z, i.e. $\chi_{final}(z) = \psi_m / (1 - \psi_m) \phi(z)$). This gives:

$$\chi_{final}(z) = \psi_m \left(1 - z / H \right)^{(\psi_m - \psi_0)/\psi_0} \qquad (4)$$

It is worth noting that this distribution (shown in Figure 2a) is independent of the drying history. From this model we can also compute a characteristic length λ, over which the final volume fraction is significant with regards to the initial volume fraction of particles. Assuming this situation is reached when the particle fraction is negligible in the rest of the sample, say when $\chi_{final}(\lambda) \approx \psi_0 / 10$, we get

$$\lambda = H \left(1 - \left(\psi_0 / (10\psi_m)\right)^{\psi_0/(\psi_m - \psi_0)}\right) \qquad (5)$$

For $\psi_0 = 5\%$ we find $\lambda = 1.4 \, \text{cm}$, which means that all the particles are essentially in the first 1.4 cm, leaving particle-free the bottom of the sample.
Now using the expression for the drying rate due to diffusion as a function of the depth of the compaction front we can solve numerically these coupled differential equations to predict the drying rate in time. The computed mass of water, integrated from the drying rate, appears to be in excellent agreement with the measures from MRI (see continuous lines in Figure 3).

CONCLUSIONS

Using a new ^{1}H MRI protocol to observe nanoparticles in an unsatured porous medium, we show that colloidal particles move towards the free surface, an effect that create a surprising heterogeneity in the solid. Since our measurements provided a detailed understanding of the physical mechanism at work we propose a simple model based on advection which predicts quite well both the distribution of particles in time and the drying rate. This suggests a technique for controlling the drying rate of porous media, by introducing an appropriate volume fraction of colloidal particle in the liquid. An important next step would be to take into account the possible interactions between colloidal particles or their adsorption on pore walls.

REFERENCES

[1] Coussot P (2000) Scaling approach of the convective drying of a porous medium. Eur. Phys. J. B 15, 557.
[2] Deegan R D, Bakajin O, Dupont TF, Huber G, Nagel S R, Witten T A (1997) Capillary flow as the cause of ring stains from dried liquid drops. Nature (London) 389, 827.
[3] Dufresne ER, Corwin EI, Greenblatt NA, Ashmore J, Wang DY, Dinsmore AD, Cheng JX, Xie XS, Hutchinson JW, and Weitz DA (2003) Flow and fracture in drying nanoparticle suspensions. Phys. Rev. Lett. 91, 224501.
[4] Faure P and Coussot P (2010) Drying of a model soil. Phys. Rev. E 82, 036303.
[5] Gauthier C, Nadji D and Coussot P (1998). Instability of the withdrawing front of a clay-water suspension slowly drying in a bead pack. C. R. Acad. Sci. Paris 326, 767.
[6] Helmig R (1997) Multiphase Flow and Transport Processes in the Subsurface. Springer, Berlin.
[7] Keita E, Faure P, Rodts S and Coussot P (2013) MRI evidence for a receding-front effect in drying porous media. Phys. Rev. E 87, 062303.
[8] Li J, Cabane B, Sztucki M, Gummel J and Goehring L (2012) Drying dip-coated colloidal films. Langmuir 28, 200.
[9] Marín A G, Gelderblom H, Lohse D and Snoeijer J H (2011) Order-to-disorder transition in ring-shaped colloidal stains. Phys. Rev. Lett. 107, 085502.
[10] Pauchard L and Allain C (2003) Buckling instability induced by polymer solution drying. Europhys. Lett. 62, 897.
[11] Pel L, Huinink H, Kopinga K, v. Hees R and Adan O (2004) Efflorescence pathway diagram: understanding salt weathering. Construction and Building Materials 18, 309.
[12] Puyate Y, Lawrence C, Buenfeld N and McLoughlin I (1998) Chloride transport models for wick action in

concrete at large Peclet number. Physics of Fluids, 10, 566

[13] Shahidzadeh-Bonn N et al. (2004) Effect of wetting on the dynamics of drainage in porous media. Transport in Porous Media 56, 209.

[14] Shahidzadeh-Bonn N, Azouni A and Coussot P (2007) Effect of wetting properties on the kinetics of drying of porous media. J. Phys.: Condens. Matter 19, 112101.

[15] Shokri N, Lehmann P, Or D (2008) Effects of hydrophobic layers on evaporation from porous media. Geophys. Res. Lett., 35, L19407

[16] Tsapis N, Dufresne ER, Sinha SS, Riera CS, Hutchinson JW, Mahadevan L, and Weitz DA (2005) Onset of buckling in drying droplets of colloidal suspensions. Phys. Rev. Lett. 94, 018302.

[17] Vendelboe A, Moldrup P, Schjonning P, Oyedele D, Jin Y, Scow K and de Jonge L (2012) Colloid release from soil aggregates: Application of laser diffraction. Vadose Zone Journal 11, 0070.

[18] Xu L, Davies S, Schofield AB and Weitz DA (2008) Dynamics of drying in 3D porous media. Phys. Rev. Lett. 101, 094502.

[19] Yiotis AG, Boudouvis AG, Stubos AK, Tsimpanogiannis IN, and Yortsos Y C (2003) Effect of liquid films on the isothermal drying of porous media. Phys. Rev. E 68, 037303.